External beam for the Heavy Ion Accelerator Facility

S. Shaharuddin[1], J. Stuchbery[1], E. C. Simpson[2,*], Z. K. Gan[1], A. C. Green[1], A. Cho[1], and E. Lu[1]

[1]Research School of Electrical, Energy and Materials Engineering, Australian National University, ACT 2601, Australia
[2]Department of Nuclear Physics, Research School of Physics, Australian National University, ACT 2601, Australia

Abstract. Radiotherapy using protons and heavier ions is emerging as an alternative to traditional photon radiotherapy for cancer treatment. Ions have a depth-dose profile that results in high energy deposition at the end of the particle's path, with a relatively low dosage elsewhere. However, the specifics of ion interactions with cellular biology are not yet fully understood. To study the induced biological effects of the ions on cell cultures, an external beam is required as biological specimens cannot be placed in vacuum. The Heavy Ion Accelerator Facility (HIAF) at the Australian National University hosts accelerators for a wide variety of ion-beam research applications. However, HIAF does not currently have an external beam capability. Here, we present an initial design for a radiobiological research capability at HIAF. A systems engineering approach was used to develop the architecture of the apparatus and determine the feasibility of adapting the current facilities to external beam applications. This effort included ion optics calculations, coupled to a Geant4 simulation, to characterise ion beam transitions through a thin window into the air. The beam spread, intensity distributions, and energy of proton and carbon ions were studied as a function of distance travelled from the window, as well as the effects of alternative window materials and thicknesses. It was determined that the proposed line at the HIAF would be suitable for the desired applications. Overall, this feasibility study lays the foundations of an external beam design, a simulation test framework, and the basis for a grant application for an external beam at the HIAF.

1 Introduction

Radiotherapy is a key component of cancer treatment. Compared to photons, radiotherapy using charged particles such as protons and carbon ions offers substantial advantages owing to its depth-dose profile, high linear energy transfer (LET) radiation, and high relative biological effectiveness [1]. Studies on ionising radiation, dosimetry, and ion induced biological effects at the molecular and cellular level are essential to improve the quality of the treatment. Such experiments are often conducted in an irradiation facility rather than a radiotherapy treatment centre.

The Heavy Ion Accelerator Facility (HIAF) at the Australian National University, Canberra supports many ion-beam research applications. The facility houses a 14UD pelletron accelerator that routinely operates above 14.5 MV. The accelerated particle beam travels to the main switching magnet before being redirected to the different beamlines. The maximum energy deliverable depends on the beam species: for protons it is ~ 29 MeV, for carbon ions ~ 100 MeV.

HIAF has plans to develop a capability for radiobiology studies. We initially studied proton and carbon ion species at energies within the HIAF's maximum capability to determine the likelihood of the facility to produce an external beam of ions. The key components for an irradiation facility for radiobiological research are a beamline that produces an external beam, a sample handling system housing the biological samples that would otherwise perish in a vacuum environment, and a dose monitoring system [2, 3]. This paper presents the initial beamline design and the sample handling system, to provide the foundation for the development of a radiobiological research application at the HIAF.

2 Simulations of the Beamline

One of the existing beamlines at HIAF is planned to be adapted for external beam applications. The beamline is an existing vacuum pipe connected from the main switching magnet in the 14UD target area, with a double quadrupole magnet, and a removable Faraday cup located in a fixed position. From the switching magnet, the beam travels in the pipe, passes the quadrupole doublet at 3.5 m downstream, and travels another 2.3 m towards the beam exit system.

For radiobiological experiments a homogeneous beam over a certain area of an irradiation field is desired. At this stage there is no hard requirement for the size of the beam spot as this is dependable on the target irradiation area. A divergent beam profile is needed to create a more uniform distribution around the central point of the beam spot. This is usually achieved by placing a scattering foil to spread the beam over an exit window area [4]. Beam optics calculations were performed using GICOSY [5] to determine the location of the beam convergence point after the quadrupole doublet.

*e-mail: edward.simpson@anu.edu.au

The beam optics calculations also determined the divergence values for the Geant4 [6] Monte-Carlo simulation of the particles traversing from the vacuum pipe, through the exit window, and into the air. This simulation aims to record the beam profile and energy at various points in the air once it transitions through the different types of exit window. This is important for determining (i) the design of the beam exit window, (ii) the distribution of the irradiation field on the target cell samples, and (iii) the optimal distance between the exit window and the target.

Within the Geant4 simulations, energy and position data were taken for z-values, i.e. the direction of beam's travel, at 2 mm increments up to 150 mm, resulting in 75 slices of the beam profile for analysis. 150 mm is chosen as the endpoint due to practical limitation on the target location. This measurement regime provides a high resolution description of the beam profile as it travels through the window matter and into the gaseous environment before reaching the target sample. The simulation was run for 15 and 25 MeV proton, and 50 and 70 MeV carbon ions against 6 μm and 10 μm Mylar, 12 μm aluminised Mylar (2 μm Aluminium), and 2.5 μm Titanium foil respectively. The results show the x- and y-position and energy of each particle at specific z-values after the exit window. The beam profiles from different test configurations were compared to determine the configuration that produces a highly uniform beam spot.

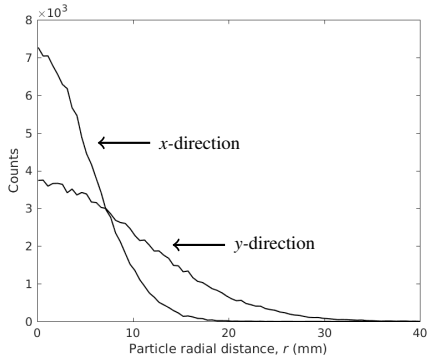

Figure 1. Radial intensity profile in the x- and y-direction for 70 MeV carbon ion beam at 150 mm in air through a 10 μm Mylar.

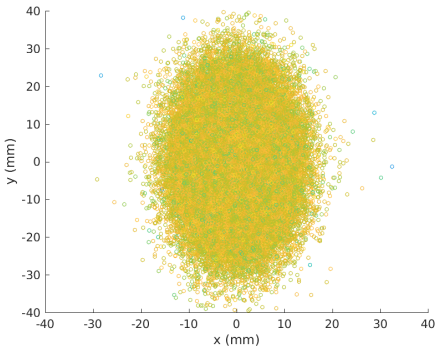

Figure 2. Two-dimensional beam profile for 70 MeV carbon ion beam at $z = 150$ mm beyond a 10 μm Mylar window.

2.1 Beam profile and radial intensity

2.1.1 Effect of the different particle types

Compared to the proton beam, the carbon ion beam spreads at a slightly larger angle and suffers much greater energy loss when traversing through the air (up to 60 MeV). The simulation of the beam profile shows that the size of the beam spot is 1 – 3 mm wider in the carbon beam. However, the increase in the divergence of the beam due to the passage through air is relatively small in both cases. After travelling 150 mm in the air, the energy of the proton beam dropped by about 3% from its initial energy, while a high energy carbon ion beam loses about 80% of the energy despite having a significantly higher initial energy than the proton beam.

The radial intensity profile for both particle types showed similar uniformity in the x- and y-directions (see Fig. 1 for carbon radial intensity profile). In general, the profile is more spread in y than x. The angular distributions calculated using GICOSY utilised a magnetic quadrupole doublet that focuses the beam asymmetrically in x- and y-directions, creating an elliptical beam spot (Fig. 2). A quadrupole triplet is required to produce a circular profile. Further work has since shown that a second quadrupole magnet located before the switching magnet may also be leveraged to provide more uniform intensity profiles along the two axes. Further simulations will determine the best approach to take.

2.1.2 Effect of the different initial beam energies

The initial beam energy for carbon ion is likely the variable that has the biggest impact for external beam irradiation. The 70 MeV carbon beam reaches the target position at $z = 150$ mm, albeit with significant energy lost, but the 50 MeV carbon beam stops in the air at $z = 96$ mm after exiting the window. Though significant loss of energy in the air is not necessarily a problem as a beam monitoring system will measure the total dose delivered to the cell sample, losses in the air could be reduced by moving the target closer to the exit window to reduce the air gap. For both accelerated carbon ion beams, the beam spot progressively expands by ~ 8 mm diameter in the air, with relatively uniform intensity distribution. For proton beams, very little loss in energy is observed due to their low charge and collision cross-section, relative to that of carbon ions. Figure 3 shows the change in energy as a function of z-distance for both proton and carbon ion beams. Note the difference in ranges on the x-axis (energy).

2.1.3 Effect of the window material

For a proton beam, the material of the exit window (Mylar, aluminised Mylar, or Ti) has very little effect on the profile

and energy of the external beam. The energy loss and angular spread are similar between the configurations. In addition, the radial intensity analysis shows minimal change in the beam uniformity as a result of different window materials, indicated by a gradual reduction in intensity as a function of the particle radial distance, r (Fig. 1). The window materials also do not affect the beam profile and uniformity in carbon ion beam. The angular spread and particle intensity distribution remains unchanged, showing good uniformity. The energy loss, though small, varies between the materials due to the their differing LET values. A finite element analysis (FEA) simulation would be required to investigate the thermal conductivity of these materials upon interaction with the ion beams.

2.1.4 Effect of the window thickness

By fixing the beam's particle type and initial energy, and the material of the window (Mylar), our simulations show minimal changes in the external beam energy and spread between 6 μm and 10 μm window thickness for a proton beam. The radial intensity distribution in the x- and y-directions are also essentially unchanged by the difference in the window thickness. For the carbon beam beam, the simulation results show consistent results in the particle angular and radial intensity distribution, with an energy loss in the thicker Mylar window of ~ 3 MeV. This is expected as the carbon ion beam has higher LET value, and so loses energy more quickly. However, we concluded that using the thicker window could (i) provide a mechanical support for the differential pressure between the vacuum and the gaseous environment, and (ii) support the thermal load dissipated by the accelerated particles. Similar to the effect of window material, these properties require further understanding using FEA techniques.

2.2 Particle energy variation as a function of the distance travelled in the air

Figure 3 shows the energy spectra for 25 MeV proton and 70 MeV carbon ion in the air after exiting the window. Note the large difference in the x-axis scales between parts (a) and (b). For the protons, the energy losses are very small (~ 0.4 MeV) and though the distribution of energies becomes broader as the beam travels further through the air, at 150 mm from the window the full-width half-maximum (FWHM) is only ~ 0.1 MeV. In contrast, the carbon ion beam suffers a much larger energy loss (~ 60 MeV) and the distribution has a FWHM of ~ 2 MeV at z = 150 mm. These losses and the associated broadening of the energy distribution must be carefully accounted for when performing biological irradiations, particularly with carbon ions.

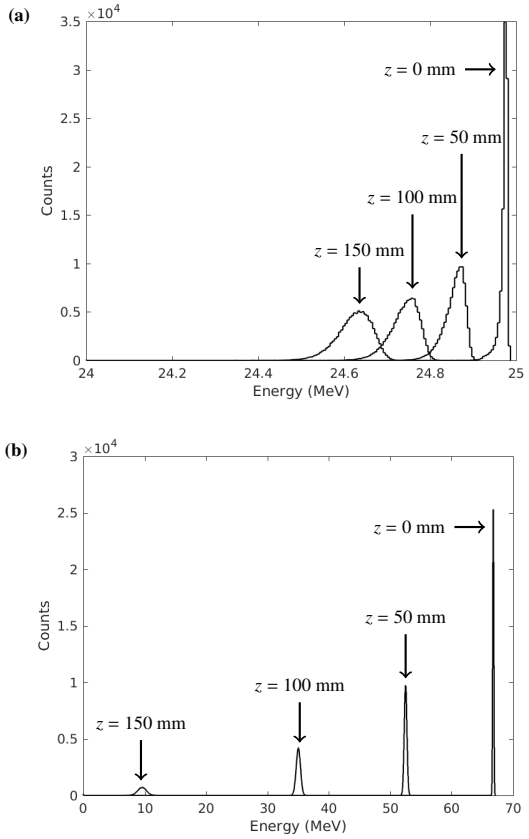

Figure 3. Energy spectrum for (a) 25 MeV proton and (b) 70 MeV carbon ion beam traversing in the air after the 10 μm Mylar exit window.

3 Design of the external beamline

This section discusses the design of the beamline itself. Figure 4 presents the schematic diagram of the proposed external beam apparatus integrated on an existing beamline. The setup includes a scattering foil, a fast-acting vacuum valve, an exit window, and a sample handling system. Similar to the design in other radiobiological irradiation facilities [3, 4, 7], the authors proposed a Au scattering foil, with thickness to be determined by simulation, placed within the existing removable Faraday cup chamber. The Faraday cup monitors the beam current and intensity in the beam pipe.

After the scattering foil and the Faraday cup, the beam passes through a high vacuum fast-acting valve, as a measure of protection in case of window rupture or failure under stress. At 0.8 m downstream from the scattering foil, the ion beam exits the pipe through a window and travels through the air gap before reaching the target. Mylar has been used as a beam exit window in some facilities [3, 7], however, we lack an FEA for its thermal conductivity and to determine the optimum thickness for HIAF application. The vertical sample holder allows for irradiation of multiple cell cultures while providing a contamination-free and temperature-controlled process. These systems are described next.

Figure 5 shows the schematic diagram of the proposed sample holder. Target cells are grown on a multiwell plate, covered with a thin Mylar sealing film to avoid (i) cross-contamination between the samples and (ii) signifi-

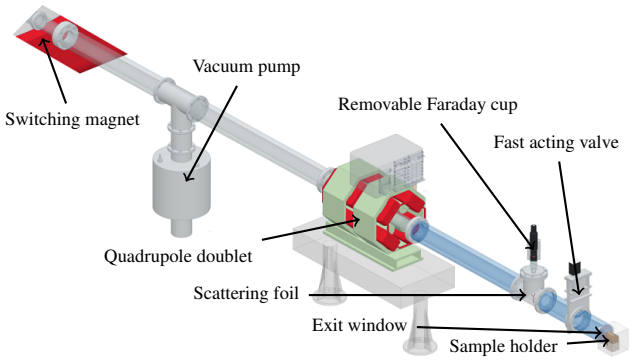

Figure 4. Schematic diagram of the proposed beamline design to produce an external beam at HIAF.

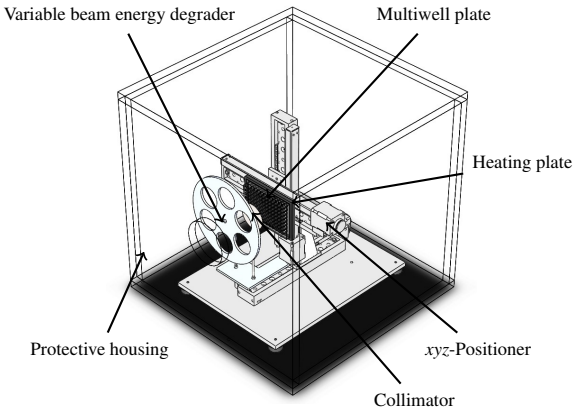

Figure 5. Schematic diagram of the sample handling system.

cant loss of the beam energy on a cell culture plate cover [8]. An *x*-*y*-*z* positioner holds the multiwell plate vertically facing the external beam and automatically positions each target cells into the beam spot using a stepper motor. The component produces a linear motion in the *x, y* and *z*-direction with *z*-axis being the direction of the beam. Positioning in the *z*-axis allows the user to move the target samples closer to the exit window and minimise the energy loss in the air by reducing the air gap. A removable heating plate is proposed to be attached to the back of the multiwell-plate for temperature control. A variable beam energy degrader using different thicknesses of Mylar foils on a circular disk manipulates the incident beam energy without changing the accelerator settings. The low-cost and readily available material ranges from 0 – 3 mm thick, aiming to reduce the beam energy by up to 50% [8]. As the beam energy reduces, the beam dispersion and uniformity will tend to increase [3]. A tantalum collimator is placed just before the multiwell plate to cut the beam size. Lastly, as a protection from the secondary particles and contamination, a polymethyl methacrylate box encloses the whole system.

4 Conclusion

A design study for an external beam at the Heavy Ion Accelerator Facility was presented, with a simulation framework that will be useful for both refinement of the design and in predicting experimental outcomes in future studies. The simulations use proton and carbon ions that travel from a vacuum beam pipe through a thin exit window into the atmospheric environment. The data recorded in the simulation show elliptical beam profiles with small differences in beam spot size dependent on the beam energy, particle type, distance from the window, and window thickness and material. The particle radial intensity distribution is fairly similar in all configurations tested, with good uniformity in the *y*-direction up to approximately 3 mm at 150 mm from the exit window. The proton beams are unaffected by the different window thickness or materials, while the carbon ion beams experienced a slight energy variation. The carbon ion beams are highly prone to energy loss in the air, especially for lower beam energies. The energy losses for the proton beams are much smaller. Sample targets may need to be placed closer to the exit window for irradiation using carbon ions. Angular spreading in both ion beams also increases as the beam particles move further from the window. Based on these beam characteristics, it is concluded that the proposed beam line is capable of supporting an external beam adaption in the future. However further work refining simulations, particular surrounding the in-pipe beam optics, and thermo-mechanical loads on the window, will be required.

Acknowledgement

We would like to thank Dr Nikolai Lobanov, Prof. Andrew Stuchbery, and Dr Lindsey Bignell from the Department of Nuclear Physics of the Australian National University, Canberra for their role and support in this project.

References

[1] D. Schardt, T. Elsässer, D. Schulz-Ertner, Rev. Mod. Phys. **82**, 383 (2010).
[2] H. Feng, L. Wu, A. Xu, B. Hu *et al.*, Cryobiology **49** (3), 241-249 (2004).
[3] N. Carlin, J. C. de Souza, E. M. Szanto *et al.*, Nucl. Instrum. Meth. A **540**, 215-221. (2005)
[4] J. Czub, D. Banas, J. Braziewicz *et al.*, Radiat. Prot. Dosm. **122**, 207-209 (2006).
[5] M. Berz, B. Hartmann, K. Lindemann *et al.*, GICOSY program, https://web-docs.gsi.de/~weick/gicosy/.
[6] S. Agostinelli, J. Allsion, K. A. Apostolakis *et al.*, Nucl. Instrum. Meth. A **506** (3), 250-303 (2003).
[7] L. Manti, L. Campajola, F. M. Perozziello *et al.*, J. Phys. Conf. Ser. **373**, 012019 (2012).
[8] J. F. Ziegler, SRIM 2013 program, http://www.srim.org/.